

# Study on Contact Force Control Characteristics of Current Collector using an Optical Sensors

Toshiaki MAKINO<sup>\*1</sup>, Takeshi KAWASAKI<sup>\*2</sup> and Muneo FURUSE<sup>\*3</sup>

## Abstract

Due to environmental problems, for a high-speed railway, such as one at 360km/h, it is particularly important to reduce the noise caused by a current collector. As a solution, a diamond-shaped low-noise current collector has been developed. However, it becomes difficult for the current collector to maintain the predetermined contact force between the contact strip and the trolley wire. Therefore, it is essential to apply an active control to keep the contact force uniform. However, there is a serious problem with the active control in that it is difficult to put sensors in the high-voltage region. In this paper, optical fiber sensors are devised and applied to the control system. In the experiment, the usefulness of the proposed sensor and control system is demonstrated for the control system.

**Key Words :** Optical Fiber Sensor, Contact Force Control, Current Collector

## 1. Introduction

Nowdays, the speed up of the railways is an international trend not only in Japan, but also in France and Germany<sup>1)</sup>. We face a serious noise problem in order to make the speed of railways more than 300 km/h. Therefore, low noise type of current collector has been developed so far. However, a number of technological developments are considered necessary before train speeds can be raised further. In Japan in particular, where Shinkansen trains run through residential areas, one of the most important issues is the development of technologies to suppress environmental noise caused by train operation<sup>2) - 3)</sup>. As a means to reduce such disturbance, a low-noise wing-type pantograph has been developed and installed on Series 500 Shinkansen Nozomi trains. However, the wing configuration of the new pantograph generates an increased lift, and its mass is approximately three times that of conventional pantographs. As a result, high-speed operation at 300km/h or more causes larger fluctuations in the contact force between pantograph contact strip and contact wire. This subsequently increases the contact loss rate, making it essential to actively control the contact

force and keep it within an allowable range<sup>4)</sup>. It is not possible, however, to install electric sensors on pantograph strips (Figure 1) since they are subjected to the high voltage of the contact wire<sup>5)</sup>. However, it is reported that the contact loss rate can be substantially reduced, if the contact force is correctly detected and actively controlled<sup>6) - 12)</sup>.

Several methods have been proposed to install multiple sensors at high-voltage points for active control of the contact force of pantograph contact strips. It has been pointed out, however, that sensors cannot be installed in high-voltage areas with present technology and, the contact force cannot directly be detected. In contrast, optical fibers (which are now enjoying increased use and are free from the influence of humidity or strong magnetic fields) can be installed just beneath the contact strips that are subject to high contact wire voltage as sensors to detect contact force<sup>13)</sup>. This enables construction of a small optical fiber sensor system that can actively control the contact force based on its output. Hence, it is considered that the contact force can be kept in an allowable range by implementing feedback control based on the measurements obtained using this system.

---

\*<sup>1</sup> National Institute of Technology, Tokuyama College

\*<sup>2</sup> Hitachi, LTD.

\*<sup>3</sup> National Institute of Technology, Oshima College

In this study, the authors devised a system whereby two compact, small-diameter plastic optical fiber (referred to below as POF) sensors are installed directly under the contact strips of the wing-type pantograph to detect the contact force acting on the strips. This detection is based on how light intensity is affected according to the external force applied. Then, the authors then used the contact force signal output by the prototype POF sensors and implemented a bench test on a prototype wing-type pantograph equipped with a servo drive mechanism to actively control the contact force. As a result, contact force fluctuations were halved when irregularities at 0.5Hz and 1.0Hz were applied to the contact wire, clearly demonstrating the effectiveness of the proposed sensing system<sup>14)</sup>.

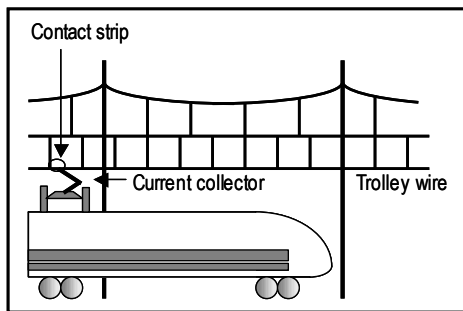


**Fig.1** Current collector system of High-speed railways

## 2. Optical fiber sensor system

### 2.1 Principle

The optical fiber-based contact force sensor system being studied works on the principle by which the propagating light intensity (i.e. the amount of transmitted light) varies according to changes in the shape of the fiber when bent or when external forces are applied. More specifically, the light intensity attenuation normally increases when the optical fiber is deformed by compressive or bending forces<sup>15)-18)</sup>. Figure 2(a) shows a sketch of a compression test on an optical fiber. When sandwiched and compressed between two plates in a radial direction (the vertical direction in Fig. 2(a)), changing its cross-sectional shape from a circle to an ellipse, the intensity of the light transmitted in the optical fiber also changes. The effect is such that the light is not redistributed in the sectional area but is partly propagated outside the fiber through the surface in contact with the plates. This in turn changes the light intensity within the optical fiber.

Figure 2(b) schematically shows the principle of

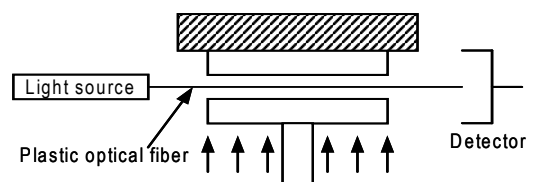
a force-detecting sensor. Equation (1) gives the fractional area loss (FAL) of light intensity when the optical fiber is deformed by a compressive force<sup>19)</sup>.

$$FAL = \frac{2}{\pi} \left\{ \arctan \left\{ \left[ \left( \frac{r}{r-\delta} \right)^2 - 1 \right]^{1/2} \right\} - \left\{ \left( 1 - \frac{\delta}{r} \right)^2 - \left( 1 - \frac{\delta}{r} \right)^4 \right\}^{1/2} \right\} \dots \dots (1)$$

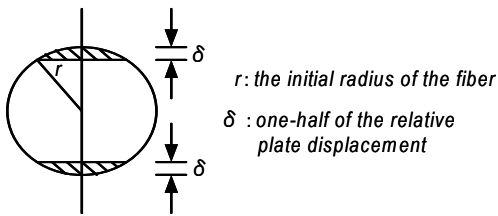
Figure 3 shows the calculated value of FAL due to geometrical changes in the optical fiber shape. Next, when an optical fiber is bent as shown in Fig. 4, the total reflection angle of the light transmitting in a mode changes on the bent waveguide so as to allow propagation of the higher order modes. Part of the light intensity in the original mode transfers to the higher modes, some of which are radiation modes. Light intensity then decreases due to this radiation loss, and a difference emerges in the propagation time between the two modes, causing deterioration in transmission characteristics. In addition, the light intensity is cut off, causing radiation loss when the critical angle becomes larger.

Where the curvature is large, the velocity at the periphery becomes higher than that at the core. Energy at the periphery is therefore thrown off at a tangent, resulting in a loss.

Since light propagates in an optical fiber from the light source to the optical detector, this force-detecting sensor can be used in places that have a high electric potential or in locations subject to electric noise (such as in strong magnetic fields), rainfall or dust. Before it can be used as a force-detecting sensor, however, it is important to clarify a number of characteristics relating to transmission light intensity.



**(a)** Experimental configuration used to investigate FAL model



(b) FAL model of a radially deformed optical fiber

Fig.2 Experimental configuration used to investigate FAL model

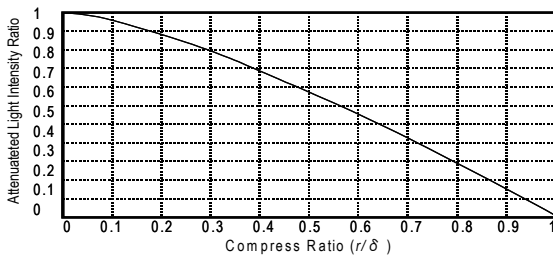


Fig.3 Relation of fractional area loss for optical fiber sensors

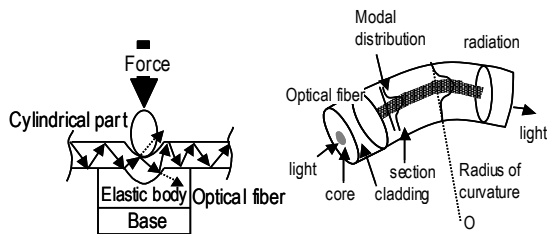


Fig.4 Principle of the optical fiber sensor micro bending loss mechanism

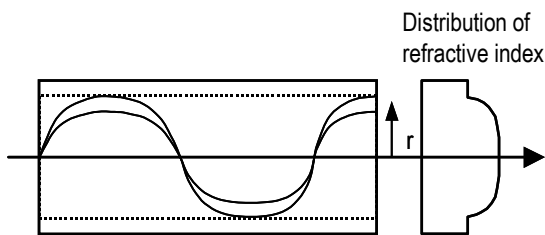


Fig.5 Configuration of the optical fiber's refractive index

## 2.2 Construction of sensor system

As optical fibers have generally been developed for use in telecommunications, they are manufactured to minimize loss in long-distance transmission and reduce the influence of external forces as much as possible. However, the force-detecting sensors used in this study need to be sensitive to external forces and have a high level of reproducibility and

reliability. This means that the difference in the refractive index between the core and the clad of the optical fiber should be small, and the mechanical properties should be improved by using the same compositions in the core and the clad. In addition, the reflection angle at the boundary between the core and the clad should be increased to give higher loss and to maximize the rate of change in light intensity due to external forces.

The optical fibers used in this study are graded index-type plastic optical fibers (POFs), referred to below as the GI type, whose refractive index gradually changes from the center to the ends. The GI-type POF has a numerical aperture of 0.20, and a refractive index of 1.508 at the center and 1.492 at the end as shown in Fig. 5.

The GI-type POF system comprises an LD light source, POF transmission lines, POF sensors, POF transmission lines, detectors and a personal computer (see Fig. 6 for system construction and Table 1 for specifications). The POF, whose core and clad are made of GI-type plastic, was developed at Keio University's Koike Laboratory. It has a numerical aperture of 0.20 and an outside diameter of 0.6mm. The wavelength and output power of the light emitted from the source are 570nm and 30mW respectively. The optical detector is a silicon APD semiconductor.

## 2.3 POF Installation

Since the prototype POFs manufactured for this study is to be installed just under the contact strip ends, they need to be compact and small in diameter (see Fig. 7). In the model used for this study, a simulated spring and damper system (or an actuator when dynamic characteristics are to be measured) is arranged on a contact strip with load cell L1 sandwiched in between. Two load cells L2 and L3 are placed under the contact strip. Each of these load cells can be replaced with a prototype POF. The POF (Fig. 8) consists of an optical fiber wound circularly, its periphery covered with a rubber sheet and a 1mm-thick circular aluminum spacer to apply distributed external force. An extra-fine aluminum rod (0.6mm in diameter) is fixed to the spacer for easy bending deformation of the POF from external forces through the rubber sheet, as well as to improve the resolution of measurement of the load characteristics. It was thus possible to reduce the size of the POFs installed just beneath the contact strip to an outer diameter of 53mm.

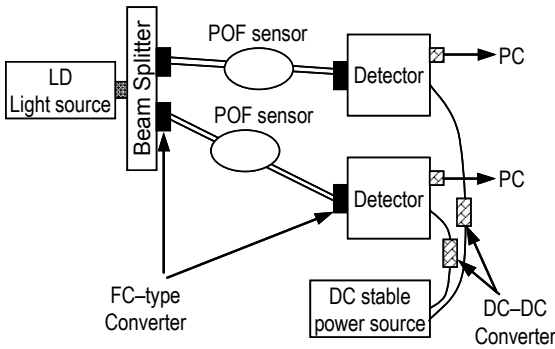


**Fig.6** Configuration of the plastic optical fiber sensor

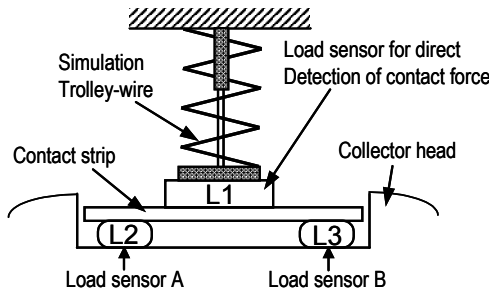


**Fig.7** Configuration of the POF

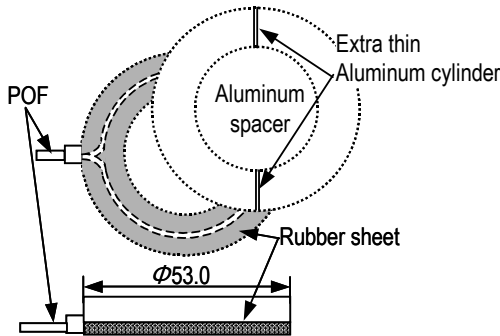


**Fig.8** Configuration of the prototype POF

**Table 1** Specification of the POF

	Item	Specification
System	Measurement range	0 – 150 N
	Accuracy resolution	15 N, 1.5N
	DC Power supply	12V, 5A, 5V
	Diameter, Weight	53mm, 30g
	Circumstance	25kV(AC),500A,130deg.
Fiber	Core, Cladding Material	Plastic(PMMA) NA=0.20, (Keio Univ., Koike Lab)
Light Source	Wave length, (Type)	570nm/30mW (Hitachi HL6726MG)
Detector	Silicon APD (Type)	200-1000nm(Peak620nm) (Hamamatsu Photo. C5460)

### 3. Shape of the prototype POF sensor and load experiment

The test apparatus (LD source, DC power source, personal computer etc.) shown in Fig. 9 was used to measure the light intensity and static load characteristics of the prototype POF sensor. Figs. 10 (a) and (b) show the measurement results.

In this test, the weight placed on the prototype POF sensor was increased up to 10kg in increments of 1kg, and the light intensity was measured by the voltage output of the optical detector and fed into a personal computer through an A/D converter. When the load was increased or decreased, the distribution of the output voltage (hysteresis) was repeatable and stable, and was in a range of about 8% as shown in Fig. 10(a).

Figure 10(b) shows the attenuation rate of the light intensity (i.e. the maximum output minus the measured output, divided by the maximum output) obtained from the static load characteristics after linear approximation. Figure 11 shows the temporal waveform obtained when a sine wave perturbation load of 15N was superimposed on a constant load of 85N using a function generator, and applied to the POF sensor with an actuator placed on the contact strip. The temporal waveforms (at 0.5Hz) of load cell L1 and POFs L2 or L3 under the contact strip present satisfactory characteristics, demonstrating that the system is able to correctly detect the contact force.

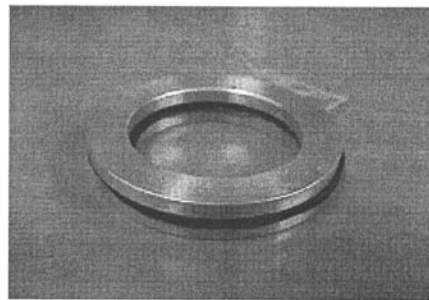


**Photo. 1** Photograph of the protptype POF sensor

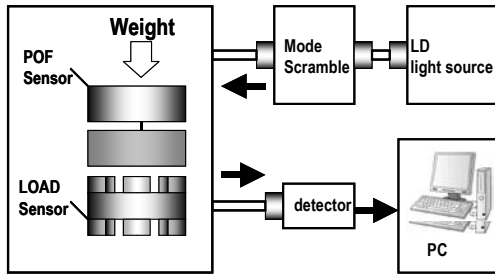
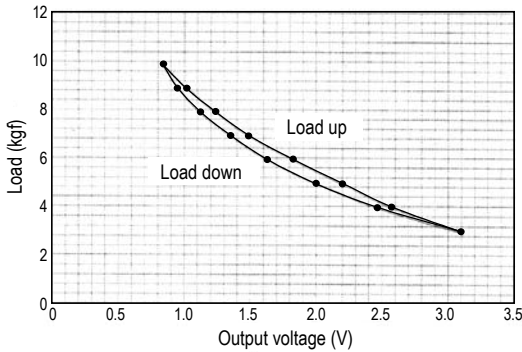
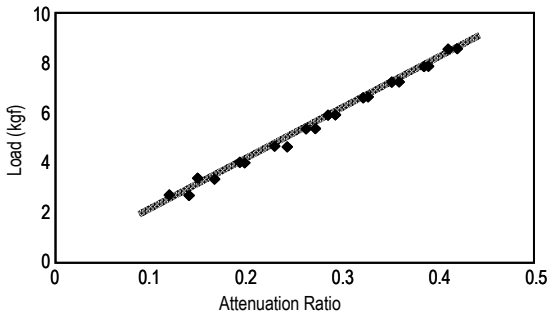


**Fig.9** Configuration of the experiment system using the POF system



(a) Relationship between output voltage and load



(b) Characteristic of relationship between load and attenuation ratio

**Fig.10** Dynamic characteristics of the prototype POF sensor

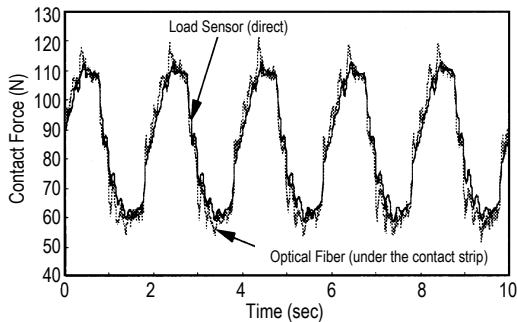


**Fig.11** Dynamic characteristic of the prototype POF sensor

## 4. Design and numerical calculation of pantograph control system

### 4.1 Design of control system

A pantograph is composed of contact strips that touch the contact wire to collect the electric power, a wing-type pantograph head equipped with a laminated spring mechanism to support the pantograph head, and insulators to support these components. Figure 12 shows the analysis model of the contact wire and pantograph system used in this study. The aforementioned POF is placed directly under contact strip m1. In the following discussion, contact loss is neglected on the assumption that the contact wire and strip remain in contact at all times. It is also assumed that the contact wire does not vibrate in the vertical direction due to car body motion. The state equation is given as

$$\begin{aligned} \dot{x}_s(t) &= A_s x_s(t) + B_{su} F_p(t) + B_{sw} d(t) + B_{st} f_{lift}(t) \\ x_s(t) &= [z_1(t) \quad \dot{z}_1(t) \quad z_2(t) \quad \dot{z}_2(t)]^T \\ d(t) &= [d(t) \quad \dot{d}(t)]^T \end{aligned} \quad \dots\dots\dots (2)$$

The frequency characteristics of contact wire irregularities caused by the intervals between support points and between hangers are assumed to be dynamic, and the disturbance in the aerodynamic upward force is also assumed to be dynamic with integration characteristics. The transfer characteristics of these disturbances are given by state equation (3).

$$\begin{aligned} \frac{d(s)}{w_d(s)} &= \frac{k_d \omega_{d1}^2 s}{(s^2 + 2\zeta_{d1} \omega_{d1} s + \omega_{d1}^2)(s^2 + 2\zeta_{d2} \omega_{d2} s + \omega_{d2}^2)} \\ \dot{x}_d(t) &= A_d x_d(t) + B_d w_d(t) \quad d(t) = C_d x_d + D_d w_d(t) \\ \dot{f}_{lift}(t) &= c_{lift} w_{lift}(t) \end{aligned} \quad \dots\dots\dots (3)$$

This equation includes the dynamic characteristics of the pneumatic servo cylinder of the control mechanism. For structural reasons, however, it is not possible to strictly determine the dynamic characteristics. Therefore, the transfer function  $G_{ac}$  from the servo amplifier input voltage  $e_i$  to the control force  $F_p$  is determined and approximated using the second order low-pass filter characteristics shown in equation (4).

$$\begin{aligned} \dot{x}_{ac}(t) &= A_{ac} x_{ac}(t) + B_{ac} e_i(t) \\ F_p &= C_{ac} x_{ac}(t) \end{aligned} \quad \dots\dots\dots (4)$$

In this approximation, frequencies over 2Hz (the follow-up limit of the pneumatic servo cylinder) were omitted. Fig. 13 shows the dynamic characteristics of the pneumatic servo cylinder. An expanded system is derived from equation (5):

$$\begin{aligned} \dot{x}_p(t) &= A_p x_p(t) + B_{pu} e_i(t) + B_{pw} w_p(t) \\ f(t) &= C_p x_p(t) + D_{pv} v(t) \end{aligned} \quad (5)$$

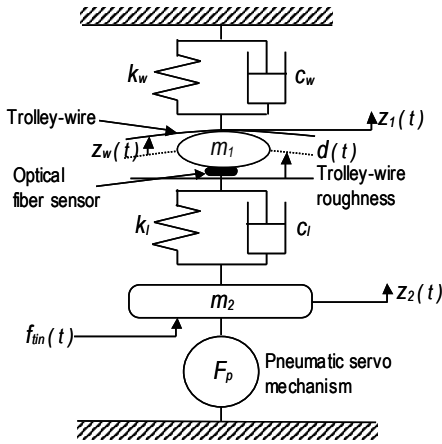


Fig.12 Analysis model of the low-noise current collector

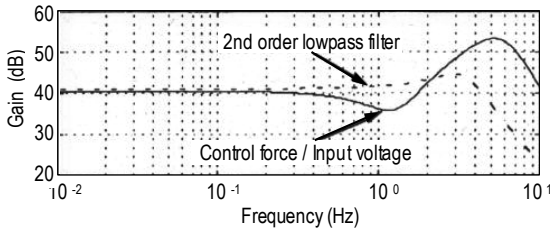


Fig.13 Characteristic of f/ ei transfer function

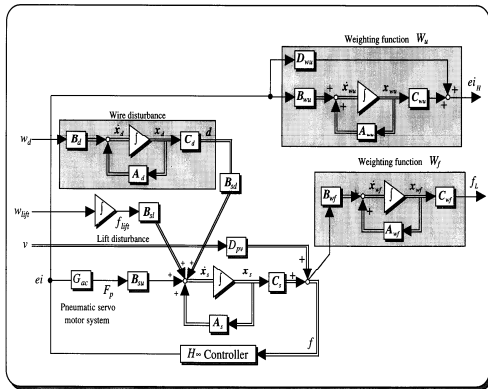


Fig.14 Generalized plant control system

A generalized plant was designed here to obtain a controller by using the weight function  $W_f(s)$  to express the second order low-pass filter suppressing contact force fluctuations in the low-frequency range, and the weight function  $W_u(s)$  to express the second order high-pass filter suppressing the control voltage in the high-frequency range (Fig. 14).

Table 2 Various parameters of low pass filter and high pass filter

Low pass filter: $W_f(s)$	High pass filter: $W_u(s)$
$L_f = 10^{(-25/20)}, \zeta_f = 0.8, \omega_f = 20 \times 2\pi$	$L_h = 10^{(-5/20)}, \zeta_h = 0.7, \omega_{uL} = 20 \times 2\pi, \omega_{uH} = 70 \times 2\pi$
Wire disturbance dynamics	Lift disturbance dynamics
$k_d = 0.9, \zeta_{d1} = 0.3, \zeta_{d2} = 0.4, \omega_{d1} = 0.5 \times 2\pi, \omega_{d2} = 9 \times 2\pi$	$C_{int} = 7$
Design parameter for $H_\infty$ control	
$\gamma = 0.9, \mu = 1 \times 10^{-10}, \epsilon = 1 \times 10^{-10}$	

4.2 Numerical calculation

Numerical calculation was performed for the pantograph in Fig. 12 using the observed values as the contact force between contact wire and strip. Figures 16 (a) and (b) show the frequency characteristics of the contact force against contact wire irregularities and against the disturbance in the aerodynamic upward force respectively.

The expanded system does not incorporate the pneumatic cylinder dynamic characteristics. Figure 15 shows the parameters of weight functions  $W_f(s)$  and  $W_u(s)$ . In the contact force between contact wire and strip detected by the POF sensor, the gain is decreased against contact wire irregularities and disturbance in the aerodynamic upward force in the frequency range of 10Hz or lower where the contact force is to be controlled. This demonstrates that the contact force can be appropriately controlled.

The frequency response of the contact force against contact wire irregularities in Fig. 16 (a) proves that fluctuations in the contact force are suppressed against irregular contact wire displacements in the low-frequency region.

The frequency response of the contact force against fluctuations in the aerodynamic upward force indicates that the fluctuations can be suppressed to -10dB or lower in a range of around 1Hz.

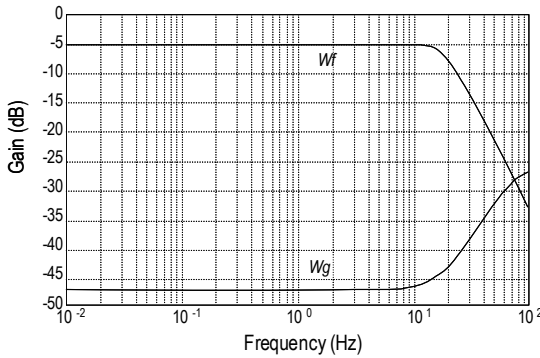
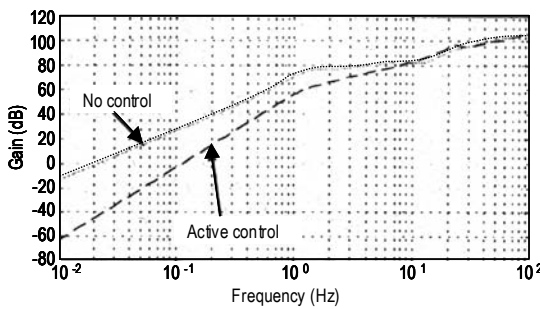
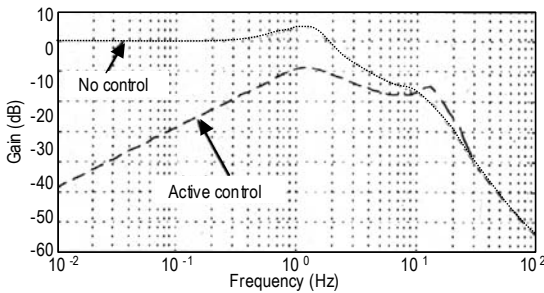


Fig.15 Characteristic of the weighting function



(a) Wire disturbance



(b) Lift disturbance

Fig.16 Frequency response of contact force

5. Control test

Photograph 2 and Fig. 17 show the appearance of the test apparatus (including the prototype pantograph) used for this study and its composition respectively. The apparatus uses springs and dampers that have the same constants as those of the heavy compound catenary system, and detects and evaluates the contact force between the spring/dampers and the prototype pantograph contact strip with load cell L1.

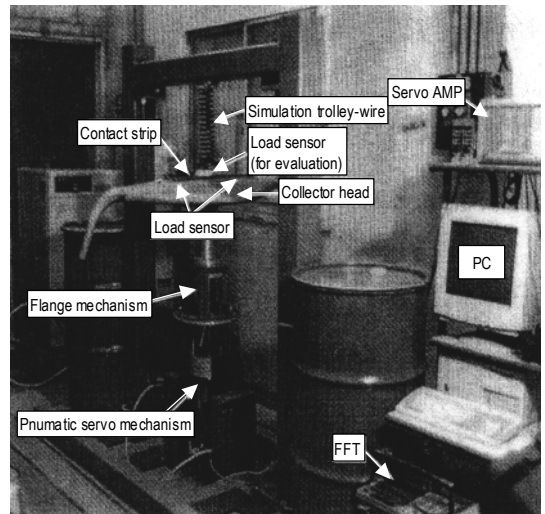


Photo.2 Photograph of the experimental apparatus

In the test, two prototype POF sensors were placed just under the contact strip to detect and control the contact force. The controller used in the test is a regulator to suppress the fluctuating component in the contact force. PI control was therefore performed to feed back the force detected by the sensor until it reached 100N, and then the controller was deployed.

Follow-up performance can be expected only up to about 2Hz for the pneumatic servo cylinder used for the control mechanism. For this reason, the transfer characteristics shown in Fig. 13 were incorporated into the expanded system when deriving the controller. Figure 18 shows the frequency response of the controller used in this test. Contact wire irregularities at about 0.5 and 1.0Hz were manually generated in the test.

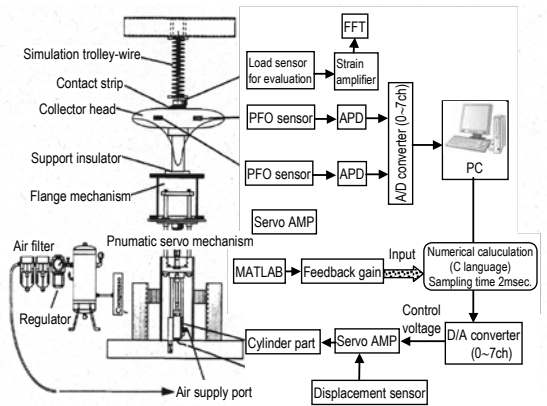
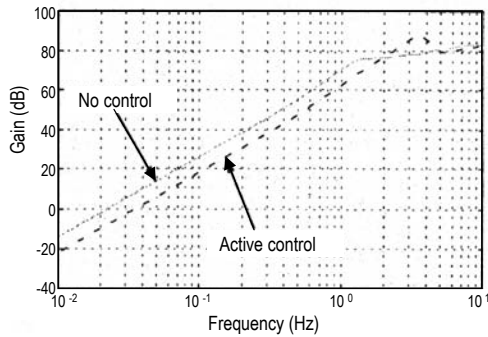
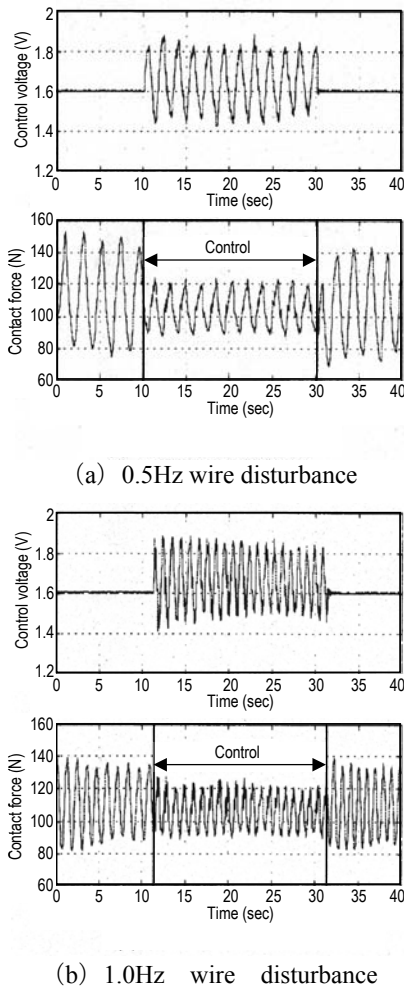


Fig.17 Schematic diagram of experimental apparatus



**Fig.18** Frequency response of contact force due to a wire disturbance



**Fig.19** Experimental result of contact force control

Figure 19(a) and (b) show the results of a test to control the contact force with POF sensors incorporated into the test pantograph. In the case of the 0.5Hz disturbance in Fig. 19(a), application of voltage to start control reduced the fluctuation in contact force from 70N to 30N. In the case of the 1Hz disturbance in Fig. 19 (b), the fluctuation decreased from 40N to 25N when control started.

These test results prove that it is possible to halve fluctuations in contact force by detection and control using two POF sensors placed under the contact strip.

## 6. Conclusions

A small-diameter POF sensors that can be placed at a high-voltage point directly under a pantograph contact strip was designed. A prototype POF was manufactured, and a method to reduce fluctuations in the contact force between contact wire and strip was proposed by active control using a controller based on the output signal of the POF sensor. The prototype POF sensors were then mounted on an actual pantograph and an active control test was performed. The results obtained from the study are summarized below.

- (1) The concept of a POF sensor that monitors light intensity attenuation characteristics against external forces applied to the plastic optical fibers was proposed. It was confirmed that the linear static load characteristics could be obtained using the sensors.
- (2) It was verified that the contact force could be directly detected using compact, small-diameter POF sensors placed directly under the pantograph contact strip.
- (3) A control test was implemented, with the result verifying the follow-up performance of the sensors against irregular contact wire displacements at 0.5Hz and 1.0Hz with a prototype pantograph using a pneumatic servo cylinder.



## References

- (1) Yoshida, K., Active Control of Low-Noise Current Collector for Super High-Speed Railways, Proc. WCRR97, Firenze 16-19, Vol.C,(1997),p.287-291
- (2) Makino, T., Trend of Active Control of Current Collector for High-Speed Railway, J.,of Fluid Power System,Vol.34, No.3(2009), p.34-38(in Japanese)
- (3) Makino T., Takehi, Y., Noise Characteristics of Current Collector for High-Speed Railways using Delta-Shaped Collector Head, Trans. Jan. Soc. Mech. Eng., Vol.63, No.612(1998),p/338-346(in Japanese)
- (4) Ohyama, T., Research and Development for Reducing Noise and Vibration in Shinkansen, RTRI Report, Vol.8, No.6 (1994), p.1-7(in Japanese)
- (5) Iida, A., Takano,Y., Makino, T., Developent of a Low-Noise Electric-Current Collector for High-Speed Trains,INTER-NOISE'94 (1994), p.163-170(in Japanese)
- (6) Yoshida, K., Seto, S., Makino, T.,Disturbance Estimation and Contact Force Control in Current Collector for High-Speed Railways, Trans. Soc. Ins. Control Eng., Vol.34,No.3 (1998), p.217-223 (in Japanese)
- (7) Yoshida, Y., Shimogo, T., A Power Collector with a Control Mechanism of Contact Force, Trans. Jan. Soc.Mech. Eng.,Vol.54,No.505 C(1988),p1821-1827(in Japanese)
- (8) Yoshida, K., Shimogo, T. and Onoda, S, Optimal Control of Vibration by Wind Force on Running Vehicle,Trans. Jan. Soc. Mech. Eng.,Vol.25,No.209,C(1982)p.70-77(in Japanese)
- (9) Thompson, A and Davis, B, An Active Pantograph with Shaped Frequency Response Dynamics, Vehicle System Dynamics, Vol.19(1990),p.131-149
- (9) Galeotti, G., Galanti, M. and magrini, S., Servo Actuated Railway Pantograph for High-Speed Running with Contact Force, Proc.Instn,Mech.Eng.Part F,Vol.207(1993), p.37-49
- (10) Namerikawa, T,Isobe, S.and Matusmura, K, H-infinity Control for Experiment Syetem of the Pantograph with a Linear DC Motor Trans. IEEJ, Vol.115, No.11 (1995), p.1412-1419(in Japanese)
- (11) Makino, T., Yoshida, K., Seto, S. and Makino, K.,Running Test on Current Colle-ctor with Contact Force Controller for High-Speed Railways, Trans. Jan. Soc. Mech. Eng. Vol.40, No.4,C(1998),p.671-680
- (12) Saeki, M., Analysis of Impact Damper with Granular Materials, Trans. of JSME, Ser.C, Vol.68, No.673(2002), p.2585-2591(in Japanese)
- (13) Yoshida, K., Ukita, M. and Makino, T., Active Compensation Control of Wind Force and Wire Roughness for Current Collector usibg Optical Fiber Sensor, Proc. ASME DETC'99MOVIC-8426(1999), p.50-56
- (14) Yoshida, K., Ukita, M. and Makino, T., Contact Force Control of Current Collector using Optical Fiber Sensor, Proc., JSME D&D Symp., No.99-7(1999), p.77-81(in Japanese)
- (15) Ishigure, T. and Koike, Y., High-Numerical Apperture Grand-Index Polymer Optical Fiber, J. of Lightwave Technology, Vol.13, No.8(1995),p.1686-1691
- (16) Muto, S., Sato, H and Hosaka, T., Optical Humidity Sensor using Fluorescent Plastic Fiber and it's Application to Breathing Condition Monitor, J. of Appl. Phys., Vol.33, No.10(1994),p.6060-6064(in Japanese)
- (17) Ito, H. and Hattori, H., Position Sensing and Communication System using Flu-Orescent Doped Plastic Fiber, J. of Appl. Phys., Vol.34, No.6, (1995),p.3109-3112(in Japanese)
- (18) Elater, J. L. and Tran.,T.A., High-Temperature Fiber Optic Strain Sensors in Fatigue Loading Conditions, SPIE, Vol.2718(1996),p.20-26
- (19) Kalymnios, D. and Rogers, I., Band Loss in Plastic Optical Fibers, Proc. of POF Conf. '97(1997),p.35-36

(Received August 29, 2014)